most of the landings occur at low descent velocities, the use of a nonlinear orifice damper in the shock absorber is preferred from the fatigue damage point of view. Viewing this in a global way, the conventional nonlinear orifice damper seems to be better than a linear damper. As the linear damper design given by Hall needs special fabrication, it appears that an optimized nonlinear orifice damper offers simplicity in design and better performance.

Acknowledgment

The author thanks A.K. Rao and R. Krishnan of the Indian Institute of Science, Bangalore, and R. Sankaranarayanan and V.T. Nagaraj of Hindustan Aeronautics Limited, Bangalore, for their encouragement and guidance in doing this work.

References

[1] Hall, H., "Some Theoretical Studies Concerning Oleo Damping Characteristics," Ministry of Technology, British Aeronautical Research Council, Current Papers, C.P. No. 951, 1967.

[2] Milwitzky, B. and Cook, F.E., "Analysis of Landing Gear Behavior," NACA TR 1154 (TN 2755), 1953.

[3] Andrews, W., Carter, A.L., Horsefall, W., and Troke, R.W., "Fatigue Test and Analysis of the F-100 Landing Gear," North American Rockwell Corporation, NA-69-535, Aug. 1969.

[4] "Airplane Strength and Rigidity: Reliability Requirements," MIL-A-8866 (ASG), May 1960.

[5] Yff, J., "Analysis of Dynamic Aircraft Landing Loads and a Proposal for Rational Design Landing Load Requirements," Ph.D. Thesis, Technische Hogeschool, Delft, June 1972.

[6] Himmelblau, D.M., *Applied Non-linear Programming*, McGraw-Hill, New York, 1972.

Computation of Two-Dimensional Potential Flow Using Elementary Vortex Distributions

Pradeep Raj* and Robin B. Gray†
Georgia Institute of Technology, Atlanta, Ga.

Nomenclature

A_{ij} = induced velocity influence coefficient
c = chord
C_p = pressure coefficient
N = number of elements on the surface
$\boldsymbol{n}$ = unit vector normal to the surface
V_∞ = freestream speed
x = chordwise coordinate
z = vertical coordinate (normal to x)
α = angle of attack
γ = intensity of elementary vortex distribution

Introduction

THE integral equation formulation using surface singularity distributions as suggested by Lamb[1] is a commonly used procedure for inviscid, incompressible flow computation on arbitrarily shaped bodies. Giesing,[2] Hess and Smith,[3] and Hess[4] utilized the source as a surface singularity; the vorticity distribution is superimposed to provide the circulation for lifting bodies. Martensen[5] and Jacob and Riegels[6] developed a procedure based on the streamfunction and used only surface-vorticity distributions. The boundary condition that the tangential velocity be zero on the inside of the profile curve leads to a Fredholm integral equation of the second kind similar to the one resulting from source distributions. Mavriplis[7] extended the same approach to single- and multielement airfoils and indicated that the surface-vorticity method may be more accurate than the surface-source method.[8] In the opinion of the authors, an important additional advantage of using vorticity is that the velocity distribution is obtained *directly* as the solution of the integral equation. Stevens et al.[9] and Woodward[10] employ vorticity as the surface singularity and implement normal-velocity boundary conditions. The profile curve of the body is approximated by an inscribed polygon composed of straight-line elements over each of which the vorticity is assumed to vary linearly. Hess[11,12] shows that this is a mathematically inconsistent higher-order implementation. His analysis indicates that the polynomial expressing the element shape should be one degree higher than that defining the surface singularity density, namely: straight-line element, constant density; parabolic element, linear distribution.

In the present investigation velocity and pressure distributions are computed on the surface of a circular cylinder and NACA basic thickness form airfoils. A second-order equation defines the profile curve of the cylinder, and the bounding surface of the airfoil is analytically represented by a higher-order expression given in Ref. 13. Surface-vorticity method coupled with zero-normal-velocity boundary condition gives a Fredholm integral equation of the first kind. An elementary vortex distribution technique which utilizes a linear distribution on each element is employed to approximate the integral equation by a set of linear algebraic equations. The resulting coefficient matrix has diagonal entries larger than other entries which is a crucial factor in numerical solution. The results presented in this note provide the detailed input vorticity distribution required by an iterative method to determine the three-dimensional flow on thick wing tips.[14]

Mathematical Model

The bounding surface is divided into a finite number of small elements each containing an unknown vorticity distribution. A simple model for the latter consists of a continuous, piecewise linear distribution with respect to the chord. All linear elementary distributions are equivalent to a set of overlapping triangular distributions. Each triangle spanning two successive surface elements is called a regular elementary vortex distribution (EVD).[15] Only one unknown, namely the vortex intensity value, γ_j, at the apex of the triangle is required for each EVD. The unknown strengths are determined by solving the system of equations

$$\sum_{j=1}^{N} A_{ij}\gamma_j = V_\infty \cdot \boldsymbol{n} \qquad (i=1,2,\ldots,N)$$

where A_{ij}, the induced velocity influence coefficient, is the normal component of induced velocity at the ith control point due to the jth EVD of unit strength. For the uniqueness of the solutions, an auxiliary condition of the total circulation around the body is specified or determined by the Kutta condition which requires zero circulation around a body for nonlifting flows. Use of symmetry about a diametric plane for the circular cylinder and the chordwise symmetry for the airfoil implicitly imposes zero circulation for nonlifting flows while simultaneously reducing the order of the coefficient matrix A. However, this also results in one more control point than the EVD stations on the surface. This problem is remedied by replacing the vorticity distribution of the surface element next to the forward stagnation point by one

Received May 25, 1978.

Index categories: Aerodynamics; Computational Methods.

*Graduate Research Assistant; presently Assistant Professor, Dept. of Aerospace Engineering, Iowa State University, Ames, Iowa. Member AIAA.

†Regents' Professor and Associate Director, School of Aerospace Engineering. Member AIAA.

Table 1 Chordwise surface velocity distribution on a circular cylinder of unit radius

	Velocity				
	Exact	Number of surface elements			
x/c	analytical	$N=72$	$N=88$	$N=108$	$N=128$
0	0	0	0	0	0
0.00025	0.0632	0.0654	0.0642	0.0654	0.0645
0.0005	0.0894	0.0915	0.0901	0.0914	0.0904
0.001	0.1264	0.1296	0.1266	0.1295	0.1275
0.005	0.2821	0.2860	0.2837	0.2858	0.2838
0.010	0.3980	0.4056	0.3973	0.4054	0.3983
0.025	0.6245	0.6322	0.6248	0.6318	0.6312
0.050	0.8718	0.8814	0.8810	0.8765	0.8766
0.10	1.2000	1.2072	1.2074	1.2017	1.2018
0.15	1.4283	1.4324	1.4325	1.4292	1.4293
0.20	1.6000	1.6029	1.6030	1.6006	1.6007
0.25	1.7320	1.7343	1.7344	1.7325	1.7326
0.30	1.8330	1.8349	1.8350	1.8334	1.8335
0.35	1.9079	1.9095	1.9096	1.9082	1.9083
0.40	1.9596	1.9611	1.9612	1.9599	1.9600
0.45	1.99	1.9914	1.9915	1.9903	1.9903
0.50	2.0	2.0014	2.0015	2.0003	2.0004
			Circulation		
	2.0	1.9994	1.99975	1.99971	1.99999

proportional to the ordinate of the surface in that region and dispensing with the control point on that small element. It should be noted that the present study uses unequal surface elements and nonuniform distribution, that is, more elements are located near the front and aft of the body where the velocity varies relatively rapidly. For lifting flows, the Kutta condition forces the vorticity strength at the trailing edge to zero. The system of linear equations is easily solved by employing Gauss-Jordan reduction using maximum pivot strategy. Additional details of the mathematical formulation and the computational techniques are described in Ref. 14.

Numerical Results

The comparison of the computed chordwise velocity distribution on a unit circular cylinder with the exact, analytical potential flow solution provides a check for the accuracy of the present method (see Table 1). For different numbers of surface elements and for different modes of distribution of elements, the computed values differ only marginally from the exact values. This is also reflected in rather insignificant differences among the values of circulation around a path enclosing the surface vorticity between the forward stagnation point and the midchord. A change in mode of distribution results in only localized variations, but increased number of elements near the front and aft stagnation points improves the agreement with the local exact values (see Table 1, $N=88$, $N=128$).

The nonlifting and lifting flows are computed for 6, 12, 18, and 24% thick NACA symmetrical airfoils. The agreement of the computed velocity distribution with the results reported by Abbott and von Doenhoff[16] is mostly within 1% based on a freestream value of unity. The chordwise pressure distributions for the 12% thick airfoil at 0 and 6 deg angles of attack are shown in Fig. 1.

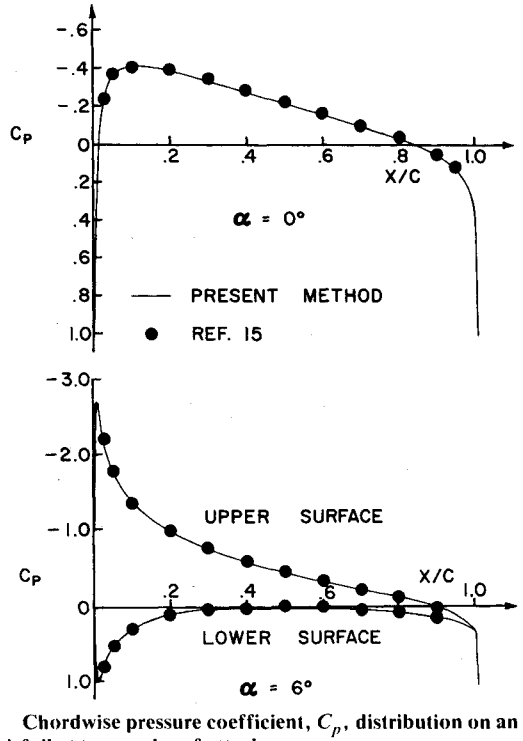

Fig. 1 Chordwise pressure coefficient, C_p, distribution on an NACA 0012 airfoil at two angles of attack.

Concluding Remarks

The two-dimensional potential flow problem is formulated using surface-vorticity distribution coupled with the conventional zero-normal-flow boundary condition. The Fredholm integral equation of the first kind, so derived, is approximated by a set of linear algebraic equations. The application of the elementary vortex distribution technique results in a coefficient matrix having dominant diagonal entries. Therefore, the equations can be easily solved by the usual numerical schemes. A continuous piecewise linear velocity distribution with respect to the chord is directly obtained as the solution of the equations. In the present study, no approximations are made to the curved shapes of the surface elements which are unequal in size and nonuniformly distributed. A measure of accuracy of the method is provided by the good agreement between the computed and the exact analytical velocity distributions for a unit circular cylinder. Nonlifting and lifting flows are computed for NACA symmetrical airfoils. The agreement of the computed results with the ones obtained by conformal transformation technique is mostly within 1%.

References

[1] Lamb, H., *Hydrodynamics*, 6th Ed., Dover Publications, Inc., New York, 1945 pp. 58-60.

[2] Giesing, J.P., "Potential Flow About Two-Dimensional Airfoils," Douglas Aircraft Co., Rept. LB-31946, Dec. 1965.

[3] Hess, J.L. and Smith, A.M.O., "Calculation of Potential Flow About Arbitrary Bodies," *Progress in Aeronautical Sciences*, Vol. 8, 1967, pp. 1-138.

[4] Hess, J.L., "Higher Order Numerical Solution of the Integral Equation for the Two-Dimensional Neumann Problem," *Computer Methods in Applied Mechanics and Engineering*, Vol. 2, Feb. 1973, pp. 1-15.

[5] Martensen, E., "Berechnung der Druckverteilung an Gitterprofilen in ebener Potentialströmmung mit einer Fredholschen Integralgleichung," *Archive for Rational Mechanics and Analysis*, Vol. 3, No. 3, 1959, p. 235.

[6] Jacob, K. and Riegels, F.W., "Berechnung der Druckverteilung endlich dicker Profile ohne und mit Klappen and Vorflügeln," *Zeitschrift fur Flugwissenschaften*, Vol. 11, 1963, pp. 357-367.

[7] Mavriplis, F., "Aerodynamic Research on High Lift Systems," *Canadian Aeronautics and Space Journal*, Vol. 17, May 1971, pp. 175-183.

[8] Mavriplis, F., "Comparison of Surface-Vorticity Method with Surface-Source Method and with an Exact Solution for Two-Dimensional Potential Flow around Two Adjacent Lifting Airfoils," *Canadian Aeronautics and Space Journal*, Vol. 19, Oct. 1973, pp. 411-413.

[9] Stevens, W.A., Goradia, S.H., and Braden, J.A., "Mathematical Model for Two-Dimensional Multi-Component Airfoils in Viscous Flow," NASA CR-1843, July 1971, pp. 21-32.

[10] Woodward, F.A., "An Improved Method for the Aerodynamic Analysis of Wing-Body-Tail Configurations in Subsonic and

Supersonic Flow, Part I—Theory and Application," NASA CR-2228, May 1973, pp. 43-46.

[11] Hess, J.L., "The Use of Higher Order Surface Singularity Distribution to Obtain Improved Potential Flow Solutions for Two-Dimensional Lifting Airfoils," *Computer Methods in Applied Mechanics and Engineering*, Vol. 5, Jan. 1975, pp. 11-35.

[12] Hess, J.L., "Review of Integral-Equation Techniques for Solving Potential-Flow Problems with Emphasis on the Surface-Source Method," *Computer Methods in Applied Mechanics and Engineering*, Vol. 5, March 1975, pp. 145-196.

[13] Jacobs, E.N., Ward, K.E., and Pinkerton, R.M., "The Characteristics of 78 Related Airfoil Sections from Tests in the Variable-Density Wind Tunnel," NACA TR 460, 1933, pp. 299-354.

[14] Raj, P., "A Method of Computing the Potential Flow on Thick Wing Tips," Ph.D. dissertation, School of Aerospace Engineering, Georgia Institute of Technology, Atlanta, Ga., 1976.

[15] Shen, C.C., Lopez, M.L., and Wasson, N.F., "Jet-Wing Lifting-Surface Theory Using Elementary Vortex Distributions," *Journal of Aircraft*, Vol. 12, May 1975, pp. 448-456.

[16] Abbott, I.H. and von Doenhoff, A.E., *Theory of Wing Sections*, Dover Publications Inc., New York, 1959, pp. 309-327.

Minimum On-Axis Noise for a Propeller or Helicopter Rotor

Martin R. Fink*
United Technologies Research Center, East Hartford, Conn.

Introduction

ONE ultimate noise floor for fixed-wing aircraft is the airframe noise caused by flow of the wing's turbulent boundary layer past the wing trailing edge. A simple method for predicting the spectrum of such noise, using known properties of turbulent boundary layers plus empirical constants, was shown[1] to predict measured flyover noise spectra of aerodynamically clean aircraft such as sailplanes and business jets.

The propeller and hovering helicopter rotor noise radiation which corresponds to airframe noise is broadband noise occurring along the rotational axis. For positions along this axis, the pressure field caused by blade loading and blade thickness is independent of azimuthal position except for fuselage interference effects on loading. Thus the only noise-producing mechanisms are lift fluctuations caused by ingestion of turbulence and airframe noise caused by the blade turbulent boundary layer and vortex wake. Ingestion of atmospheric turbulence was shown[2] to be an important cause of on-axis propeller noise in static operation. This mechanism should be unimportant for helicopter rotors, which have much smaller disc loadings, and becomes less important for propellers as forward speed is increased. There is interest in predicting the ultimate limits on noise from thrusting propulsive devices. Such a prediction method could be obtained from that which had been developed for fixed-wing airframes and evaluated by comparisons with available data.

As shown herein, spectra calculated by a strip-theory equivalent of the method developed for fixed-wing airframe noise generally matched those measured with a thrusting helicopter rotor. They overpredicted the spectra of a non-thrusting propeller, which is a fault caused by overprediction of noise radiation from nonlifting airfoils.

Received June 13, 1978.

Index categories: Noise; Propeller and Rotor Systems; Aeroacoustics.

*Senior Consulting Engineer, Aerodynamics. Associate Fellow AIAA.

Prediction Method

An exact equation exists[3] for the noise radiated when one turbulent eddy of known size and intensity is convected past a sharp trailing edge. It was shown[1] that an equation having this analytically derived form, and an empirically determined amplitude, matched available data for peak overall sound pressure level (OASPL) and flyover directivity pattern of aerodynamically clean airframes. This amplitude factor was further adjusted to provide separate predictions of trailing edge noise from the wing and horizontal tail and was given as Eq. (10) of Ref. 1. For an unswept trailing edge, and free-field levels rather than those for a microphone in the presence of ground reflection, this is

$$\mathrm{OASPL} = 50\log(V/100\,\mathrm{m/s}) + 10\log(\delta b/R^2) + 10\log(\cos\phi\cos\theta/2)^2 + 113.9\,\mathrm{dB} \quad (1)$$

where V is the relative velocity and δ is the boundary-layer thickness at the trailing edge of the mean geometric chord as calculated for a flat-plate turbulence boundary layer

$$\delta = 0.37\,c(Vc/\nu)^{-0.2} \quad (2)$$

Also b is the span, R is the far-field distance, ϕ is the sideline angle, θ is the direction angle relative to the chord line, c is the chord, and ν is the kinematic viscosity. The free-field 1/3 octave spectrum in the absence of atmospheric attenuation was given by Eq. (7) of Ref. 1

$$\mathrm{SPL}_{1/3} - \mathrm{OASPL} = 10\log\{0.613(f/f_{\max})^4[(f/f_{\max})^{3/2} + 0.5]^{-4}\} \quad (3)$$

where $f_{\max}$, the frequency at maximum amplitude is given by

$$f_{\max} = 0.1\,V/\delta \quad (4)$$

These equations were applied to calculation of noise along the rotational axis of rotating blades. Each blade was regarded as comprised of a large number of radial segments, each with constant relative velocity $V_T\,r/r_T$. Here r is the average radius at the segment, and the subscript T denotes the blade tip. Then $R^2 = X^2 + r^2$ and $\phi = \cos^{-1} r/X$, where X is the distance along the axis of rotation from the blade disc plane to the microphone, and θ can be calculated from local blade twist and pitch angle. Span b of each radial segment should be taken as the product of segment span and number of blades. The spectra calculated for different radial segments can be added to give the complete spectrum.

This calculation method was implemented numerically for the simple case of two constant-chord blades at a great distance (relative to tip radius) from the measurement point. Blade twist and airfoil camber were neglected. Then c, R, ϕ, and θ were independent of radial position, with $10\log(\cos\phi\cos\theta/2)^2$ taken equal to -3 dB.

Calculations were conducted of noise on the rotational axis two diameters from a two-blade propeller with 3.05-m diameter and 0.424-m chord, at 136 m/s tip speed. Inboard radial extent of the blade was varied to permit examination of noise contributed by different radial regions. These spectra are plotted in Fig. 1. The outer 10% of the blade is predicted to radiate more than half the noise (within 3 dB of the total) at frequencies above that for peak amplitude. Except for frequencies more than three octaves below the peak-amplitude frequency, essentially all the broadband noise is predicted to come from the region beyond 60% of the tip radius.

Comparisons with Data

Spectra are available[4] for an unusual propeller with the dimensions assumed above. This propeller had 0.045 rad (2.57